

Impact of Phyllosilicates on Amino Acid Formation under Asteroidal Conditions

V. Vinogradoff,* L. Remusat, H. L. McLain, J. C. Aponte, S. Bernard, G. Danger, J. P. Dworkin, J. E. Elsila, and M. Jaber



Cite This: *ACS Earth Space Chem.* 2020, 4, 1398–1407



Read Online

ACCESS |



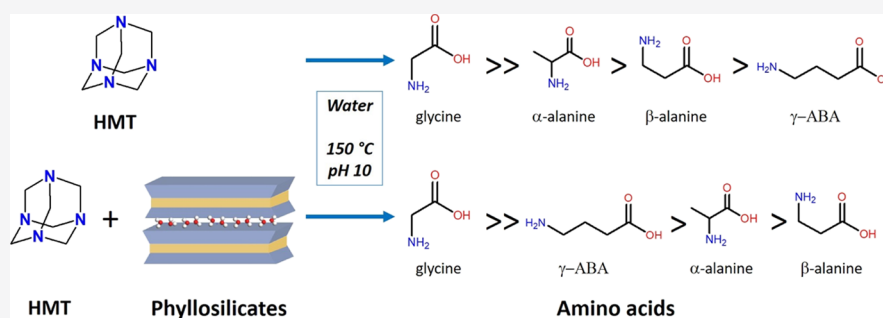
Metrics & More



Article Recommendations



Supporting Information



ABSTRACT: The emergence of life on Earth could have benefitted from an extraterrestrial source of amino acids. Yet, the origin of these amino acids is still debated because they may have formed prior to the solar nebula or inside the parent body of meteorites. Here, we experimentally produced amino acids by exposing an interstellar model molecule (hexamethylenetetramine) to asteroid-like hydrothermal conditions (150 °C; pH 10). We conducted additional experiments in the presence of carboxylic acids and phyllosilicates to simulate asteroidal environments. Analyses via liquid chromatography–mass spectrometry show that glycine is the most abundant amino acid formed, but non-proteinogenic α -, β -, and γ -amino acids are also produced. This production of amino acids seems to be hampered by the presence of Fe-rich smectites, while the presence of Al-rich smectites largely stimulates it. Our findings evidence (1) the production of amino acids during hydrothermal alteration of a putative interstellar precursor, (2) the importance of the formose reaction from formaldehyde and ammonia, for amino acid synthesis in meteorites, and (3) the impact of organic–mineral interactions on the nature/distribution of the amino acids produced. Altogether, the fact that the production of amino acids, which are so central to living structures, can be achieved via organo–mineral interactions under hydrothermal conditions should put these processes at a focal point for research on the origin of extraterrestrial organic compounds and into the origin of life.

KEYWORDS: amino acids, hydrothermal reactions, smectite, asteroid, hexamethylenetetramine

1. INTRODUCTION

Amino acids are among the most interesting compounds in extraterrestrial organic matter because of their irreplaceable role in all Earth life systems. These organic compounds are present in non-negligible quantities in carbonaceous chondrites (–up to 300 ppm in CR2);^{1–5} however, their abiotic origins are still a subject of debate. The synthesis of most amino acids is believed to have occurred during hydrothermal processes happening inside the parent body of meteorites, from accreted precursors such as aldehydes, cyanide, ketones, and ammonia.^{2,5,6} Current theories propose that significant amounts of meteorite organic matter, or its precursors, can be first formed in an interstellar environment, such as on icy grains by irradiation and heating processes and then during the protosolar nebula phase.⁷ This heritage is supported by isotopic studies showing noticeable enrichment in heavy stable isotopes of C, N, and H in chondritic organics, including

amino acids,⁸ likely originating from energetic processing at low temperatures (<50 K) during precursor formation.⁹ From these precursors, different chemical pathways are proposed to elucidate amino acid formation during hydrothermal alteration inside asteroids: the Strecker reaction that produces α -amino acids, the Michael addition to produce β -amino acids, and the decarboxylation of α -amino dicarboxylic acids as a possible formation of γ - and δ -amino acids. Amino acid analyses highlight that the degree of alteration in different parent bodies influences the relative molecular distribution of α , β , γ -, and δ -

Received: May 20, 2020

Revised: July 16, 2020

Accepted: July 16, 2020

Published: July 17, 2020



amino acids.⁵ For example, higher degrees of thermal alteration have been linked to higher abundances of *n*- ω -amino acids;¹⁰ in contrast, less aqueously altered carbonaceous chondrites contain higher abundances of α -amino acids, as seen in the Paris meteorite,¹¹ which is considered one of the least altered CM carbonaceous chondrites.¹² Nonetheless, these trends are not always valid and may reflect different compositions of precursor compounds accreted by the parent body, rather than significant differences caused by aqueous or thermal alterations. Indeed, disparities and diversities in amino acid distribution appear within carbonaceous chondrite groups presenting similar petrological types and alteration degrees,² suggesting other chemical processes, such as local mineral–organic interactions occurring within the asteroid parent body. Carbonaceous chondrites contain >95 wt % minerals, and the impact of these mineral phases on the formation of amino acids during hydrothermal alteration is currently poorly constrained. Therefore, more experimental studies are required to decipher pathways leading to the formation of amino acids in carbonaceous asteroids during hydrothermal alteration.

Here, we investigate the formation of amino acids under asteroidal conditions from hexamethylenetetramine (HMT). HMT is a molecule representative of the evolution of ices from the interstellar medium (ISM) to the solar nebula,¹³ and we assume that it could have been accreted on primitive small bodies. Laboratory experiments simulating interstellar ices can reproduce the primary processes affecting the organic matter formed in the ISM and the following transformations of the ices during protoplanetary disk evolution toward the solar nebula. These experiments show that from ices composed of simple molecules such as methanol, ammonia, and water, a refractory organic residue, called a protoplanetary residue, made of thousands of species, is produced after processing by ultraviolet irradiation and warming (10–300 K).^{13–15} Among molecules formed in the protoplanetary residue, HMT is of primary interest because it is thermodynamically favored during the warming of the ices (it can remain stable at 130–230 °C at low pressure in the solid phase) and can represent 50% of the protoplanetary residue (as evidenced by infrared spectroscopy).^{13,14,16–19} Previous studies have shown that HMT can form amino acids (up to 50 μ M concentrations) when subjected to acidic hydrolysis.²⁰ It is also worth mentioning that the analyses, by hydrolysis, of such protoplanetary residues are known to detect amino acids (up to 50 nM; glycine being the most abundant species found).^{21–25}

The formation of amino acids is likely influenced by multiple parameters on the parent bodies: nature of the organic and mineral phases, pH, concentration of reactants, temperature, oxidation state, water to rock ratio, and duration of aqueous alteration.² In this study, we focus on the influence of the nature of organic and mineral phases and the duration of the aqueous alteration. We evaluate the synthesis and molecular distribution of aliphatic amino acids during the hydrothermal processing of HMT alone or when mixed with carboxylic acids (CAs) or in the presence of phyllosilicates in alkaline solutions (pH 10) with heating at 150 °C for different duration, mimicking hydrothermal alteration conditions.²⁶ CAs are some of the most abundant organic compounds observed in carbonaceous chondrites.⁴ Phyllosilicates are the main hydrated minerals in the matrices of carbonaceous chondrites.^{26–28} Furthermore, phyllosilicates can exert strong interaction with organic molecules²⁹ and have shown intimate

association with organic matter in various chondrite groups.^{30–32} In this work, we compare the impact of two synthetic smectites of different compositions: (i) a montmorillonite, an aluminum–magnesium-bearing smectite (Al-rich smectite), with well-known properties toward organic–mineral associations^{33–35} and (ii) a nontronite, an iron-bearing smectite (Fe-rich smectite), to investigate the roles of the smectite composition and properties, regarding the synthesis of amino acids. Analysis by liquid chromatography coupled to mass spectrometry (MS) (with fluorescence detection) was performed on the sample, without a hydrolysis step, to reveal the free amino acids produced in the experiments.

2. MATERIALS AND METHODS

2.1. Synthesis of Phyllosilicates. Synthetic phyllosilicates were used to prevent undesirable organic contamination. They are smectites from the same synthesis batch as the ones used in our previous studies.³⁶ The synthesis used bulk chemicals (silica, aluminum, magnesium, and iron) processed via hydrothermal synthesis following a well-tested method by Jaber et al.^{35,37} and Andrieux and Petit.³⁸ Briefly, dioctahedral Al-rich 2:1 smectites were synthesized by mixing deionized water, hydrofluoric acid (HF, Sigma-Aldrich, 40%), sodium acetate (Sigma-Aldrich, 99%), magnesium acetate tetrahydrate ($\text{Mg}(\text{CH}_3\text{CO}_2)_2 \cdot 4\text{H}_2\text{O}$, Sigma-Aldrich, 99%), and Al and Si salts. HF was used to reach a higher crystallinity.³⁹ The hydrogel was kept for 2 h at room temperature and then introduced into a poly-(tetrafluoroethylene)-lined stainless-steel autoclave [polytetrafluoroethylene (PTFE) reactor] and heated at 200 °C for 72 h. Products were recovered by filtration, washed thoroughly with distilled water, and dried at 60 °C for 12 h. The empirical formula per half unit cell (mainly determined by X-ray fluorescence) is similar to montmorillonite: $\text{Na}_{0.3}(\text{Mg}_{0.3}\text{Al}_{1.7})\text{Si}_4\text{O}_{10}(\text{OH}_{1.5}\text{F}_{0.5}) \cdot n\text{H}_2\text{O}$, hereafter called Al-rich smectite. This phyllosilicate is called Al-rich smectite in this work. The Fe-rich 2:1 smectite was synthesized by mixing sodium metasilicate (Na_2SiO_3 , Sigma-Aldrich, 50–53% SiO_2), aluminum chloride (AlCl_3 , Sigma-Aldrich, 98%), iron chloride (FeCl_3 , Sigma-Aldrich, 97%), and magnesium chloride (MgCl_2 , Sigma-Aldrich, 98%). The average composition measured by a multi-technical approach, including Mossbauer and X-ray fluorescence, is $\text{Na}_{0.42}(\text{Al}_{0.18}\text{Fe}_{1.80}\text{Mg}_{0.02})(\text{Si}_{3.60}\text{Al}_{0.38}\text{Fe}_{0.02})\text{O}_{10}(\text{OH})_2 \cdot n\text{H}_2\text{O}$, hereafter called Fe-rich smectite. Detailed methods for the characterization of the synthetic smectites by infrared and X-ray diffraction are presented in [Supporting Information](#) (Figure SI1).

2.2. Experimental and Analytical Procedures. **2.2.1. Experimental Setup.** Our experimental protocol has been described previously for the analysis of HMT under hydrothermal conditions.^{36,40} To prepare the experimental mixtures, solutions were prepared: a pH = 10 solution of double-distilled water with KOH (10^{-4} M) degassed with argon (hereafter called alkaline solution) and a CA solution made of formic (Sigma-Aldrich, 95%), acetic (Sigma-Aldrich, 99.7%) and propionic (Sigma-Aldrich, 99.5%) acids, at 6 M equal concentration, adjusted to pH = 5 using KOH pellets and degassed with argon (hereafter called CA solution). For mixtures containing HMT-only, 100 mg of HMT powder (Sigma-Aldrich >99%) was dissolved in 1 mL of the alkaline solution to obtain a concentration of 0.7 M, which is below the saturation point of HMT in water (6.1 M at 25 °C). For mixtures containing HMT and CA, 100 mg of HMT powder was added with 120 μ L of the CA solution and 0.88 mL of the

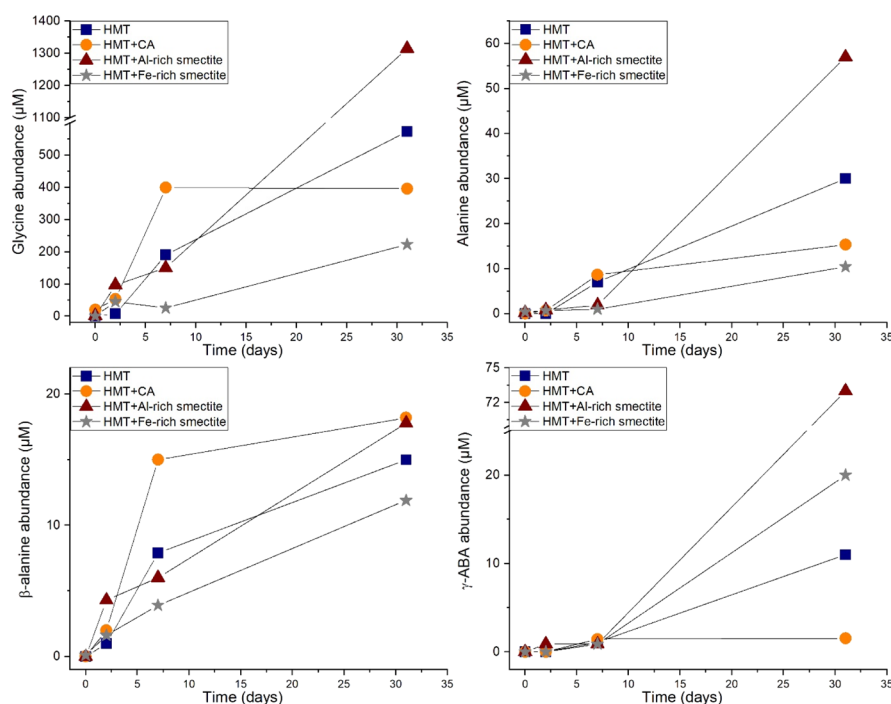


Figure 1. Evolution of glycine, alanine, β -alanine, and γ -ABA abundances formed with time in the four different hydrothermal experiments at 150 °C from HMT, HMT + CA, HMT + Al-rich smectite, and HMT + Fe-rich smectite. Values are the average of three measurements from single-ion liquid chromatograms as detailed in the [Materials and Methods](#) section; standard deviations are smaller than the symbols and are not shown here ([Table S11](#)).

alkaline solution to obtain equal concentrations of HMT and CA (i.e., 0.7 M). For the mixture containing smectite, 100 mg of synthetic phyllosilicate was added in the reactor with 100 mg of HMT and 1 mL of the alkaline solution. These mixtures were prepared under an argon atmosphere (>99.999%; Air Liquide, ALPHAGAZ 1) in a glove box (<0.5 ppm O₂) and loaded into sealed 23 mL PTFE reactors. Reactors were then put in an oven with temperature accurately regulated at 150 °C for 2, 7, or 31 days in closed systems ($P \geq 6$ bars based on the vapor pressure of water, note that ammonia, formaldehyde or other products formed from HMT can also increase the pressure). At the end of the experiments, the pH (measured on pH paper) values ranged between 8 and 9 for all the mixtures. Each hydrothermal reactor was thoroughly cleaned prior to experiments with different solvents (water, methanol), then left for at least 2 days in water at 150 °C, dried, and finally heated empty for some days at 150 °C.

After the completion of the experiments, the reactors were opened in air and the mixtures were transferred from the reactors to Eppendorf tubes (Biopur certified PCR clean) and centrifuged (2 mL, 6 min at 12,000 rpm). The soluble compounds were hence separated from the solid³⁶ or the insoluble macromolecular carbon.⁴⁰ Half of the final water solution was used for liquid–liquid extraction with dichloromethane and gas chromatography–MS (GC–MS) analysis (reported previously).⁴⁰ The other half was used in the analyses to search for amino acids.

Starting mixtures (0 day), representing the control experiment in [Table S11](#), are the starting materials mixed together, stirred, and left for 24 h at 25 °C in a closed Eppendorf (Biopur). Then, the 0 day samples are treated the same way as the hydrothermal experiments (centrifuged, washed with solvents, and dried).

2.2.2. Sample Procedure for Amino Acid Analysis. Samples were diluted to 200 mM HMT, and 10 μ L of aliquots of that concentration were dried down with 20 μ L of sodium borate (0.1 M) buffer pH = 9 to evaporate any amines that were present in the samples. Each dried residue was brought up in 10 μ L of water, and then 20 μ L of Waters AccQ:Tag derivatizing agent and 70 μ L of AccQ:Tag sodium borate buffer were added. Standards consisting of a set of 9 calibrators of amino acids (0.25–250 μ M) were prepared in water and treated in the same way (see [Table S12](#) for a complete list of amino acid standards). Both samples and standards were heated for 10 min at 55 °C immediately following the addition of the derivatizing agent. The samples were then analyzed via the commercial Waters AccQ:Tag protocol on a Xevo G2 XS time of flight mass spectrometer equipped with an electrospray ionization source (positive ion mode), a mass resolution setting of 5000 $m/\Delta m$ but without external mass accuracy calibration. The Xevo G2 XS electrospray capillary voltage was set to 0.8 keV, the sampling cone was set to 30 °C, the source temperature was set to 120 °C, the cone gas flow was set to 70 L/h, the desolvation temperature was set to 500 °C, and the desolvation gas flow was set to 1000 L/h. Samples were introduced via a Waters Acquity UHPLC with a fluorescence detector. For UHPLC analysis, a 250 μ L syringe, 50 μ L loop, and 30 μ L needle were used. The total injection volume was 1 μ L. Selected amino acid ion traces were quantitated. A linear least-square model was fitted to each proteinogenic amino acid in the standard calibration set, and these calibration curves were used to quantify the analytes in the samples. For the nonproteinogenic amino acids, the relative instrument responses for these analytes compared to alanine were calculated using calibration standards prepared and analyzed at a later date, and these responses were used together with the alanine calibration curve to quantify these compounds in the

samples. A procedural blank sample, that is, a sample of pure water that has undergone the same preparation and analytical procedures, was used to determine procedural and laboratory backgrounds. Samples were analyzed in triplicate.

This method is robust and rapid and has been used for many studies (see e.g., refs^{41–43}). The insensitivity to dissolved salts⁴⁴ permits the analysis of samples without the need for prederivatization desalting; however, the fluorescent product is not a diastereomer and does not permit chiral separation of amino acids, seen in other methods.⁴⁵

3. RESULTS

Four sets of experiments were implemented to evaluate the formation of amino acids: HMT-only, HMT with CAs (CA; formic, acetic, and propionic acids), HMT with Al-rich smectite, and HMT with Fe-rich smectite. Each experiment was running under hydrothermal alteration conditions at 150 °C and pH 10 for 0, 2, 7, and 31 days (Figure 1; see Materials and Methods section for experimental details). The 0-day samples represent the analysis of the starting materials; for most of these mixtures at 0-day, the amounts of amino acids are near detection limits (Table S11), demonstrating no glycine contamination in the minerals or the HMT standard. However, glycine contamination is observed at 0 day in the HMT + CA experiment, indicating contamination from the CA standards purchased from Aldrich (see Materials and Methods) (Figure 1). After 31 days of hydrothermal conditions, the total concentration of amino acids produced ranges from 270 to 1470 μM (Figure 2, Table S11). Glycine is the most abundant

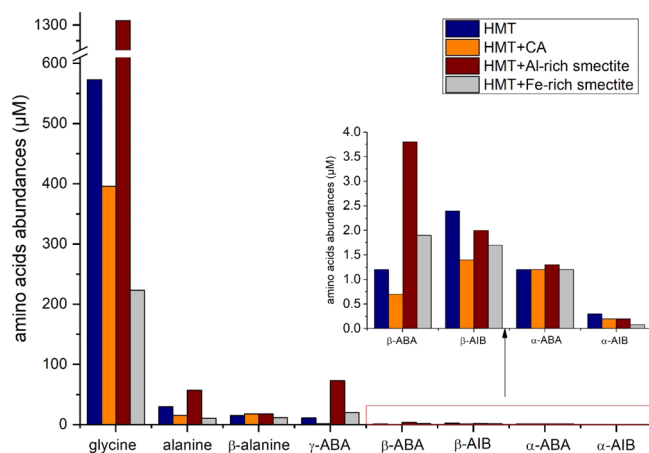


Figure 2. Bar graph showing the abundance of the amino acids formed after 31 days of hydrothermal reaction at 150 °C in the experiments from HMT, HMT + CA, HMT + Al-rich smectite, and HMT + Fe-rich smectite. (Analytical error bars are not represented, see Table S11).

amino acid produced in all experiments, and it represents around 90% of the total amino acids formed (Figures 1, 2, and S12). Its abundance increases with time in all experiments except for HMT + CA for which it remained constant between 7 and 31 days ($\sim 400 \mu\text{M}$; Figure 1). Overall, after 31 days, the highest amount of glycine produced is obtained for the HMT + Al-rich smectite experiment ($\sim 1300 \mu\text{M}$ glycine).

After glycine, the most abundant amino acids are alanine, β -alanine, and γ -aminobutyric acid (γ -ABA) (Figure 2.). Only trace amounts of α - and β -aminoisobutyric acid (AIB) and α - and β -ABA are observed (Figures 2, S12), and with a few

exceptions (in the HMT + CA experiments), there is a clear overall increase with time of the abundances of these amino acids in our experiments (Figure 1). In the HMT-only experiment, the amino acid abundances after 31 days of hydrothermal reaction are inversely correlated with the amino acid molecular weights [glycine (C2) \gg α -alanine (C3) > β -alanine (C3) > γ -ABA (C4) concentrations; Figure S11, Table S12]. This trend is not consistent in the rest of experiments; HMT + CA resulted in similar concentrations of α - and β -alanine and a lower production of γ -ABA (glycine \gg alanine \approx β -alanine \gg γ -ABA), while HMT + Al-rich and HMT + Fe-rich smectites resulted in molecular distributions which favored the formation of γ -ABA (C4) over α - and β -alanine (C3) (Figure S12, Table S12). The HMT + Al-rich smectite reaction exhibited the highest concentration of γ -ABA and the highest total production of amino acids after 31 days, 1470 μM , which is more than twice the abundance of amino acids from HMT-only (Figure 2, Table S11). Noted that the glycine to alanine ratio is consistent at about 20 in all experiments. The mixtures containing CA present their peak in amino acid production after 7 days (Figure S13, Table S13). No proteinogenic amino acids other than glycine and alanine were detected, despite being targeted for analysis in our samples and procedural blanks (Figure S13, Table S13); it thus indicates that biological contamination can be ruled out in our experiment.

4. DISCUSSION

4.1. Mechanism of Amino Acid Formation from HMT

Alone. Our study reveals that amino acids can form in modest abundances, 0.04–0.2 yield % (Table S12), during 31 days of hydrothermal evolution of HMT (0.7 M, 150 °C, and pH 10). Previous analyses of these experiments have shown that a complex network of chemical reactions took place.^{36,40} The chemical reaction mechanism that we propose starts from HMT dissociation into formaldehyde and ammonia, which leads to the condensation of formaldehyde (formose reaction) occurring in parallel to the amine–sugar reactions (Maillard-type reactions). These two reactions result in a rich molecular diversity, dominated by low mass nitrogen-bearing molecules such as aliphatic amines (e.g., methylamine and dimethylamine), nitrogen heterocycle (e.g., pyrazine, imidazole, and pyrimidine), amides (e.g., *N,N*-dimethyl-formamide), and high molecular weight molecules ($m/z > 140$) known as soluble melanoidins.^{46–48} Note that from hydrothermal alteration of HMT-only, insoluble melanoidins were also produced.⁴⁰ In presence of phyllosilicates,³⁶ previous investigations revealed a lower diversity of free organic product extract in solvent (dichloromethane), with fewer high molecular-weight species. Analyses conducted on the smectite residues displayed the entrapment of organic molecules within the smectites, including ammonium ions (at least 7 wt % of organic matter).³⁶

Here, the detected amino acids might derive from formaldehyde and ammonia generated by HMT degradation. Because of the absence of a cyanide source in the initial mixture and the unfavorable chemical conditions to form nitriles from formaldehyde and ammonia under our hydrothermal conditions,^{49,50} the Strecker cyanohydrin synthesis may be inactive for the formation of α -amino acids in this work. Our results hence indicate that the formose reaction in the presence of ammonia should be considered as the main reaction mechanism leading to the formation of the amino acids in our experiments.^{48,51–53} The inclusion of ammonia in

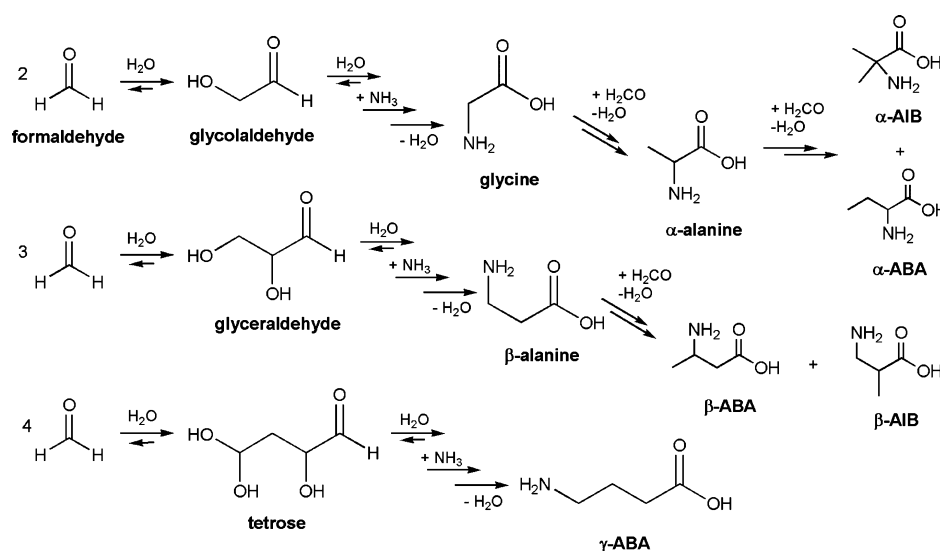


Figure 3. Putative pathways for the formation of the observed amino acid distribution from HMT decomposition (producing formaldehyde and ammonia) via the formose reaction and the sugar model. The first step is the polymerization of formaldehyde in water corresponding to the formose reaction.

the formose reaction (also known as the sugar model) has been shown to form glycine through the reaction of glycolic acid with ammonia^{48,54} (Figure 3). Alanine is expected in lower abundances than glycine because its formation occurs by the addition of formaldehyde to glycine;^{48,53,54} which is in agreement with the similar glycine/alanine ratio (~ 20) in our experiments after 31 days of reactions. β -Alanine is the product of the reaction between glyceraldehyde and ammonia,⁵⁵ while γ -ABA may be formed from tetrose precursors reacting with ammonia, according to the sugar model pathways.⁴⁶ Additional formaldehyde additions can lead to the formation of α -AIB and α -ABA but in rather low concentrations⁵³ (Figure 3). Because the formose reaction with ammonia can explain the most abundant amino acids detected in our experiments, we suggest that this is the main synthetic pathway for the formation of amino acids from HMT (Figure 3). This mechanism is consistent with previous experiments starting from formaldehyde and ammonia. Indeed, the relative abundances and molecular distributions of amino acids from the HMT-only reaction are similar to those found in formaldehyde–ammonia–glycolaldehyde systems.^{48,54,56} In this later system, the reaction is relatively faster with a highest production of alanine (alanine \gg glycine $>$ β -alanine $>$ γ -ABA) likely due to the initial presence of glycolaldehyde as starting reagent and the use of $\text{Ca}(\text{OH})_2$, known as formose reaction catalysts,^{46,57,58} unlike our experiments in which HMT was the only starting reactant.

In addition, previous investigations have shown that the Maillard reaction model⁴⁷ added to the formose reaction led to an increase in chemical reactivity and molecular diversity,⁴⁰ and thus, several routes could have occurred in parallel to the formaldehyde and ammonia reaction in our reaction network to produce amino acids. The non-proteinogenic *n*- ω -amino acids (i.e., β -alanine and γ -ABA) may be the ring-opening decomposition products of aliphatic lactams produced from Maillard-like reactions. The production of lactams, such as methyl-pyrrolidinone observed by GC–MS in our previous work,^{36,40} could then induce a larger production of γ -ABA.⁵⁹ Therefore, this reaction mechanism may explain the late formation of γ -ABA (production sharply increases after 7 days

of reaction, Figure 1), given that lactams would have to form first, before hydrolyzing into amino acids in our reaction network.

4.2. Impact of Carboxylic Acids and Smectites on the Production of Amino Acids. Experiments including CAs as part of the starting mixtures, exhibit a plateau in the production of the four main amino acids studied here after seven days of reaction (Figure 1). Except for β -alanine, a lower abundance of amino acids was even observed from these samples after 31 days of reaction. The yield of amino acids in these experiments is only 66% of that of the 31 days HMT-only experiment (Figure 2, Table SII). Two main reasons can be proposed for these observations. First, the formose and Maillard-like reactions compete with the nucleophilic addition of an amine to a CA to produce amides.^{60–62} The formation of amides has been observed on non-targeted GC–MS analyses of HMT + CA experiments, reported in Supporting Information (see Supporting Information). Aliphatic amides are formed after two days of experiments (Figures SI4, SI5, Table SI4). At the beginning of the hydrothermal reaction (before 7 days), the presence of CA seems to accelerate the formation of glycine, alanine, β -alanine, and γ -ABA compared to HMT-only experiments (Figure 1, Table SII); however, the drop in concentration of ammonia and amines caused by reaction with CAs for the formation of amides may hamper the production of larger amounts of amino acids. Second, because of the presence of CA and the production of amides, the pH of the mixture may have varied through the course of the experiments. Indeed, the large production of amides during the first days, which are neutral species (pH ~ 7), could have reduced optimum conditions for the formose reaction between 2 and 7 days. The formose reaction is favorable in alkaline pH,⁴⁶ and thus, a decrease of the pH could stop the production of amino acids. Nonetheless, this should have been transitory because the pH of the 7 days HMT + CA sample ranges between 8 and 9.

In the presence of smectites, the distribution of amino acids changed, most notably for γ -ABA. We propose that γ -ABA may be produced either by the formose reaction or by lactam ring-opening; thus, it might be possible that the smectites used here

favored the production of tetroses⁶³ or the lactam ring-opening, enhancing the formation of γ -ABA over α - and β -alanine and the α - and β -ABA isomers. Previously, we have observed that the negatively charged surface of our smectites (edge and interlayer space) can adsorb positive or polar compounds such as sugars or ammonium derivatives.³⁶ The surfaces of smectites, especially montmorillonites, are also known to favor the production of peptides and sugars.^{64,65} The Al-rich smectite used in our experiments may have similar properties to those of montmorillonite, which may explain the higher abundance of amino acids and particularly of γ -ABA from HMT (Figure 2). Although the chemical interactions between the molecules and the smectite are difficult to fathom,³⁶ the formose reaction is known to be sensitive to and catalyzed by multivalent cations (typically Ca^{2+}).⁵⁸ In our previous analyses on the smectite residues leftover after 31 days of hydrothermal alteration with HMT,³⁶ we noted the partial transformation of the Al-rich smectite into kaolin phyllosilicates ($\text{Al}_2\text{Si}_2\text{O}_5(\text{OH})_4$). Such mineral transformations for the Al-rich smectite have undoubtedly leached some Mg^{2+} and Al^{3+} in the solution, which could have acted as a catalyst of the formose reaction. This may explain the twice higher production of amino acids in the HMT + Al-rich smectite samples compared to HMT alone. The smectite residues, reported previously,³⁶ also present an increase of the interlayer spacing of the phyllosilicate structure, especially in the Fe-rich smectite hydrothermal residue after 31 days of reactions.³⁶ By infrared spectroscopy, we identified ammonium cations (NH_4^+), likely indicating an exchange between Na^+ and NH_4^+ (also in the Al-rich smectite samples), and so the release of Na^+ in the solution. The chemical composition of our Fe-rich smectite remaining unchanged, the presence of Na^+ in the solution seems to be not sufficient to catalyze the formose reaction and the production of amino acids (because the abundance of amino acids formed in the Fe-rich smectite mixture are the lowest). Further experiments are needed to validate such cation effects (Mg^{2+} or Al^{3+} or Na^+) on the formose/ammonia reaction under hydrothermal conditions. In addition, two other factors can be discussed for the samples with Fe-rich smectites showing the lowest total amino acids production, with γ -ABA remaining the second most abundant amino acid formed (Table SI2). First, the Fe-rich smectite has a specific surface area ($42 \text{ m}^2/\text{g}$) twice as small as the Al-rich smectite ($77 \text{ m}^2/\text{g}$),³⁶ thus probably adsorbing less compounds than the Al-rich smectite. Second, previous elemental analysis, infrared and X-ray spectroscopy analyses, showed a higher content in N atoms adsorbed in the Fe-rich smectite, mainly related to ammonium/amine cations.³⁶ These latter ions could be strongly adsorbed on the negative Fe-rich smectite layers because of the higher negative charge induced by iron located in both tetrahedral and octahedral layers, compared to aluminum ions located only in octahedral layers in the Al-rich smectite.^{29,36} In this case, the surface would be saturated hence not available for enhancing the formose/ammonia reactions.

These results using smectites and HMT show a manifest link between the chemical composition of the mineral and the production of amino acids, as well as on the C3–C4 amino acid/glycine ratio (Table SI2, Figure 1).

4.3. Implications for the Origin of Extraterrestrial Amino Acids in Meteorites. Amino acids in extraterrestrial samples have been investigated for decades because of their potential implication in the origin of life; nevertheless, their

formation and evolution in carbonaceous chondrites remain contentious. Our observations show that the formose reaction with ammonia, or sugar model, should be considered as a potential synthetic pathway to meteoritic amino acids. While the formose/ammonia reaction is known to lead to amino acids in aqueous environments on Earth,^{48,51} it has not been proposed for extraterrestrial amino acid formation yet. We especially highlight that α - and n - ω -amino acids can be formed from this formose with ammonia reaction (Figure 3) and not only from the Strecker cyanohydrin and Michael addition reactions. Hence, the combination of all these reactions and the diverse suite of organic precursors accreted in asteroids may account for the large diversity and abundance of amino acids in carbonaceous chondrites, such as Murchison, Orgueil,⁶⁶ and Paris.¹¹ The Paris meteorite, the least aqueously altered CM chondrite,⁶⁷ is particularly depleted in amino acids compared to Murchison (CM), which could reinforce the importance of the aqueous alteration for the formation of amino acids inside the meteorite parent bodies.¹¹ Note that extensive hydrothermal alteration or heating is also known to alter and decrease the abundance of amino acids.² Moreover, the production of some amino acids can also reach a maximum after some time of hydrothermal alteration, as observed with HMT + CA experiments and then decrease if the alteration continues; thus, some amino acids may therefore be only intermediates in a complex chemical network.

While some studies point to the diversity of the organic precursors to explain amino acid variations, the role of the mineral phases during hydrothermal alteration has been barely considered.⁶⁸ Organic matter and minerals are intimately associated in the chondrite matrices,^{12,30–32,69} and their co-evolution during hydrothermal alteration has now been proposed by several authors.^{12,30–32,36,70} The present experiments suggest that smectites have a significant impact on the nature and abundance of amino acids formed during hydrothermal alteration of HMT. This may be due to the different adsorption capacity and reactivity of smectites, which favor different chemical pathways. In light of our study, the peculiar distribution of the C4 amino acids such as γ -ABA, analyzed in a wide range of carbonaceous chondrites,⁵ can be interpreted in part as the result of the mineral phase composition. While the most abundant meteoritic minerals are phyllosilicates, iron-oxides, sulfates, or carbonates co-exist in meteorites and could also potentially affect the formation of amino acids.⁶⁸ The variable mineralogy of the parent bodies can explain the diverse distribution of amino acids, even considering the hypothesis of the accretion of common precursors among carbonaceous chondrite groups. In addition, hydrothermal alteration occurs mainly in microlocalized environments within the parent body,^{30–32,70,71} which may create independent local surroundings where different reactions with minerals could have occurred. Analysis of amino acid distributions at the same scale as the hydrothermal alteration could allow the observation of larger variability in the amino acid distribution in carbonaceous chondrites.

The large enrichment in deuterium (D) observed for the amino acids in carbonaceous chondrites (δD values ranging from +180 to +3419‰ for amino acids in Murchison)^{8,72–74} may relate them to interstellar precursors such as HMT. This statement is based on the high D/H fractionation process occurring at low temperatures in cold interstellar environments, where different molecules (e.g., methanol, formaldehyde, and ammonia) are known to be enriched in D.^{9,75}

This scenario suggests a direct continuity between molecules formed in the course of ISM evolution to the solar nebula and the molecules analyzed in carbonaceous chondrites. Deuterated HMT, formed from D-rich molecules in interstellar ices,⁷⁶ could have been accreted on the parent bodies of meteorites and hence would have resulted in D-rich amino acids. Further experiments are planned to investigate this D-rich signature upon evolution of the organic matter in different environments, including in carbonaceous chondrites during hydrothermal alteration.

5. CONCLUSIONS

Our study reveals that α -, β -, and γ -amino acids can be synthesized from the hydrothermal alteration in asteroid conditions of HMT, a molecule produced during the evolution of interstellar ice analogues. While amino acid synthesis in extraterrestrial samples was commonly explained by the Strecker cyanohydrin and Michael addition reactions that require hydrogen cyanide or nitrile sources, we propose that these amino acids may also be formed via the formose reaction with ammonia and Maillard-type reactions. These reactions are induced by formaldehyde and amines, produced from the decomposition of HMT, a potential precursor accreted in the parent body. We further observed the impact of minerals and CAs on the distribution and abundance of amino acids in our experimental simulation. We highlight the impact of the nature of smectites, which can hamper (Fe-rich smectite) or stimulate (Al-rich smectite) the formation of amino acids. More investigations on organic–mineral interactions are under progress to improve the understanding of amino acid formation and more widely to organic matter in extraterrestrial environments. Besides meteorites, this pioneering work opens new opportunities for the search of amino acids in prebiotic terrestrial and extraterrestrial environments, such as Mars, by giving first indications on the suitable mineral environment for amino acid formation from hydrothermal alteration of simple universal molecules (formaldehyde and ammonia).

■ ASSOCIATED CONTENT

SI Supporting Information

The Supporting Information is available free of charge at <https://pubs.acs.org/doi/10.1021/acsearthspacechem.0c00137>.

Infrared spectra and X-ray diffraction spectra, abundance of amino acid analyzed, amino acid yields, bar graph of the nature and distribution of the amino acids formed, fluorescence chromatogram, list of amino acid and their abundance, and list of amide compounds found in the HMT+CA mixtures and their mass spectra (PDF)

■ AUTHOR INFORMATION

Corresponding Author

V. Vinogradoff – CNRS, Aix-Marseille University, Physique des Interactions Ioniques et Moléculaires, PIIM UMR 7345, ASTRO Team, 13013 Marseille, France; Muséum National d'Histoire Naturelle, Sorbonne Université, UMR CNRS 7590, Institut de Minéralogie, de Physique des Matériaux et de Cosmochimie, 75005 Paris, France; orcid.org/0000-0003-4107-0980; Email: vassilissa.vinogradoff@univ-amu.fr

Authors

L. Remusat – Muséum National d'Histoire Naturelle, Sorbonne Université, UMR CNRS 7590, Institut de Minéralogie, de Physique des Matériaux et de Cosmochimie, 75005 Paris, France

H. L. McLain – Solar System Exploration Division, NASA Goddard Space Flight Center, Greenbelt, Maryland 20771, United States; Department of Chemistry, The Catholic University of America, Washington, D.C. 20064, United States

J. C. Aponte – Solar System Exploration Division, NASA Goddard Space Flight Center, Greenbelt, Maryland 20771, United States; Department of Chemistry, The Catholic University of America, Washington, D.C. 20064, United States; orcid.org/0000-0002-0131-1981

S. Bernard – Muséum National d'Histoire Naturelle, Sorbonne Université, UMR CNRS 7590, Institut de Minéralogie, de Physique des Matériaux et de Cosmochimie, 75005 Paris, France

G. Danger – CNRS, Aix-Marseille University, Physique des Interactions Ioniques et Moléculaires, PIIM UMR 7345, ASTRO Team, 13013 Marseille, France; Institut Universitaire de France (IUF), 75231 Paris Cedex 05, France

J. P. Dworkin – Solar System Exploration Division, NASA Goddard Space Flight Center, Greenbelt, Maryland 20771, United States; orcid.org/0000-0002-3961-8997

J. E. Elsila – Solar System Exploration Division, NASA Goddard Space Flight Center, Greenbelt, Maryland 20771, United States

M. Jaber – Institut Universitaire de France (IUF), 75231 Paris Cedex 05, France; Sorbonne Université, CNRS UMR 8220, LAMS, 75252 Paris Cedex 05, France; orcid.org/0000-0001-7772-1023

Complete contact information is available at:

<https://pubs.acs.org/doi/10.1021/acsearthspacechem.0c00137>

Author Contributions

V.V., L.R., S.B., and M.J. conceived research; M.J. synthesized the phyllosilicates; V.V. designed and performed experiments; V.V. and H.L.M. performed UHPLC analysis. H.L.M. performed data treatment, helped by J.P.D., J.E.E., J.C.A., and V.V.; V.V. wrote the first version of the manuscript and all authors contributed to the final manuscript.

Notes

The authors declare no competing financial interest.

■ ACKNOWLEDGMENTS

This research was funded by the program Emergences Ville de Paris (PI: L.R.), the MNHN ATM program (PI: V.V.), a grant from the Simons Foundation (SCOL award 302497 to J.P.D.), and support from the NASA Astrobiology Institute through award 13-13NAI7-0032 to the Goddard Center for Astrobiology for H.L.M., J.C.A., J.E.E., and J.P.D. This work was also supported by the Programme National de Planétologie (PNP) of CNRS/INSU, co-funded by CNES (PI V.V.). L.R. is grateful to the European Research Council for funding via the ERC project HYDROMA (grant agreement no. 819587). We are grateful to anonymous reviewers for their helpful comments.

■ REFERENCES

(1) Burton, A. S.; Stern, J. C.; Elsila, J. E.; Glavin, D. P.; Dworkin, J. P. Understanding Prebiotic Chemistry through the Analysis of

Extraterrestrial Amino Acids and Nucleobases in Meteorites. *Chem. Soc. Rev.* **2012**, *41*, 5459–5472.

(2) Glavin, D. P.; Callahan, M. P.; Dworkin, J. P.; Elsila, J. E. The Effects of Parent Body Processes on Amino Acids in Carbonaceous Chondrites. *Meteorit. Planet. Sci.* **2010**, *45*, 1948–1972.

(3) Martins, Z.; Sephton, M. A. Extraterrestrial Amino Acids. In *Amino Acids, Peptides and Proteins in Organic Chemistry*; Hughes, A. B., Ed.; Wiley-VCH Verlag GmbH & Co. KGaA, 2009; pp 1–42.

(4) Pizzarello, S.; Cooper, G. W.; Flynn, G. J. The Nature and Distribution of the Organic Material in Carbonaceous Chondrites and Interplanetary Dust Particles. *Meteorites and the Early Solar System II*; University of Arizona Press, 2006; pp 625–651.

(5) Elsila, J. E.; Aponte, J. C.; Blackmond, D. G.; Burton, A. S.; Dworkin, J. P.; Glavin, D. P. Meteoritic Amino Acids: Diversity in Compositions Reflects Parent Body Histories. *ACS Cent. Sci.* **2016**, *2*, 370–379.

(6) Aponte, J. C.; Elsila, J. E.; Glavin, D. P.; Milam, S. N.; Charnley, S. B.; Dworkin, J. P. Pathways to Meteoritic Glycine and Methylamine. *ACS Earth Space Chem.* **2017**, *1*, 3–13.

(7) Caselli, P.; Ceccarelli, C. Our Astrochemical Heritage. *Astron. Astrophys. Rev.* **2012**, *20*, 20–56.

(8) Elsila, J. E.; Charnley, S. B.; Burton, A. S.; Glavin, D. P.; Dworkin, J. P. Compound-Specific Carbon, Nitrogen, and Hydrogen Isotopic Ratios for Amino Acids in CM and CR Chondrites and Their Use in Evaluating Potential Formation Pathways. *Meteorit. Planet. Sci.* **2012**, *47*, 1517–1536.

(9) Roueff, E.; Gerin, M. Deuterium in Molecules of the Interstellar Medium. *Space Sci. Rev.* **2003**, *106*, 61–72.

(10) Chan, H.-S.; Martins, Z.; Sephton, M. A. Amino Acid Analyses of Type 3 Chondrites Colony, Ornans, Chainpur, and Bishunpur. *Meteorit. Planet. Sci.* **2012**, *47*, 1502–1516.

(11) Martins, Z.; Modica, P.; Zanda, B.; d'Hendecourt, L. L. S. The Amino Acid and Hydrocarbon Contents of the Paris Meteorite: Insights into the Most Primitive CM Chondrite. *Meteorit. Planet. Sci.* **2015**, *50*, 926–943.

(12) Vinogradoff, V.; Le Guillou, C.; Bernard, S.; Binet, L.; Cartigny, P.; Brearley, A. J.; Remusat, L. Paris vs. Murchison: Impact of Hydrothermal Alteration on Organic Matter in CM Chondrites. *Geochim. Cosmochim. Acta* **2017**, *212*, 234–252.

(13) Bernstein, M. P.; Sandford, S. A.; Allamandola, L. J.; Chang, S.; Scharberg, M. A. Organic Compounds Produced by Photolysis of Realistic Interstellar and Cometary Ice Analogs Containing Methanol. *Astrophys. J.* **1995**, *454*, 327–344.

(14) Muñoz Caro, G. M.; Schutte, W. A. UV-Photoprocessing of Interstellar Ice Analogs: New Infrared Spectroscopic Results. *Astron. Astrophys.* **2003**, *412*, 121–132.

(15) Danger, G.; Orthous-Daunay, F.-R.; de Marcellus, P.; Modica, P.; Vuitton, V.; Duvernay, F.; Flandinet, L.; Le Sergeant d'Hendecourt, L.; Thissen, R.; Chiavassa, T. Characterization of Laboratory Analogs of Interstellar/Cometary Organic Residues Using Very High Resolution Mass Spectrometry. *Geochim. Cosmochim. Acta* **2013**, *118*, 184–201.

(16) Vinogradoff, V.; Rimola, A.; Duvernay, F.; Danger, G.; Theulé, P.; Chiavassa, T. The Mechanism of Hexamethylenetetramine (HMT) Formation in the Solid State at Low Temperature. *Phys. Chem. Chem. Phys.* **2012**, *14*, 12309–12320.

(17) Vinogradoff, V.; Fray, N.; Duvernay, F.; Briani, G.; Danger, G.; Cottin, H.; Theulé, P.; Chiavassa, T. Importance of Thermal Reactivity for Hexamethylenetetramine Formation from Simulated Interstellar Ices. *Astron. Astrophys.* **2013**, *551*, A128.

(18) Briggs, R.; Ertem, G.; Ferris, J. P.; Greenberg, J. M.; McCain, P. J.; Mendoza-Gomez, C. X.; Schutte, W. Comet Halley as an Aggregate of Interstellar Dust and Further Evidence for the Photochemical Formation of Organics in the Interstellar Medium. *Origins Life Evol. Biospheres* **1992**, *22*, 287–307.

(19) Vinogradoff, V.; Duvernay, F.; Fray, N.; Bouilloud, M.; Chiavassa, T.; Cottin, H. Carbon Dioxide Influence on the Thermal Formation of Complex Organic Molecules in Interstellar Ice Analogs. *Astrophys. J.* **2015**, *809*, L18.

(20) Hulett, H. R.; Wolman, Y.; Miller, S. L.; Ibanez, J.; Orò, J.; Fox, S. W.; Windsor, C. R. Formaldehyde and Ammonia as Precursors to Prebiotic Amino Acids. *Science* **1971**, *174*, 1038–1041.

(21) Bernstein, M. P.; Dworkin, J. P.; Sandford, S. A.; Cooper, G. W.; Allamandola, L. J. Racemic Amino Acids from the Ultraviolet Photolysis of Interstellar Ice Analogues. *Nature* **2002**, *416*, 401–403.

(22) Muñoz Caro, G. M.; Meierhenrich, U. J.; Schutte, W. A.; Barbier, B.; Arcones Segovia, A.; Rosenbauer, H.; Thiemann, W. H.-P.; Brack, A.; Greenberg, J. M. Amino Acids from Ultraviolet Irradiation of Interstellar Ice Analogues. *Nature* **2002**, *416*, 403–406.

(23) Nuevo, M.; Auger, G.; Blanot, D.; d'Hendecourt, L. A Detailed Study of the Amino Acids Produced from the Vacuum UV Irradiation of Interstellar Ice Analogs. *Origins Life Evol. Biospheres* **2008**, *38*, 37–56.

(24) Meinert, C.; Filippi, J.-J.; de Marcellus, P.; Le Sergeant d'Hendecourt, L.; Meierhenrich, U. J. N-(2-Aminoethyl) Glycine and Amino Acids from Interstellar Ice Analogues. *ChemPlusChem* **2012**, *77*, 186–191.

(25) Modica, P.; Martins, Z.; Meinert, C.; Zanda, B.; d'Hendecourt, L. L. S. The Amino Acid Distribution in Laboratory Analogs of Extraterrestrial Organic Matter: A Comparison to CM Chondrites. *Astrophys. J.* **2018**, *865*, 41.

(26) Brearley, A. J. The Action of Water. *Meteorites and the Early Solar System II*; University of Arizona Press, 2006; pp 584–624.

(27) Garenne, A.; Beck, P.; Montes-Hernandez, G.; Chiriac, R.; Toche, F.; Quirico, E.; Bonal, L.; Schmitt, B. The Abundance and Stability of “Water” in Type 1 and 2 Carbonaceous Chondrites (CI, CM and CR). *Geochim. Cosmochim. Acta* **2014**, *137*, 93–112.

(28) Howard, K. T.; Alexander, C. M. O. D.; Schrader, D. L.; Dyl, K. A. Classification of Hydrous Meteorites (CR, CM and C2 Ungrouped) by Phyllosilicate Fraction: PSD-XRD Modal Mineralogy and Planetesimal Environments. *Geochim. Cosmochim. Acta* **2015**, *149*, 206–222.

(29) Lagaly, G.; Ogawa, M.; Dékány, I. Clay Mineral–Organic Interactions. In *Handbook of Clay Science*; Bergaya, F., Lagaly, G., Eds.; Developments in Clay Science; Elsevier, 2013; Chapter 10.3, Vol. 5, pp 435–505.

(30) Le Guillou, C.; Bernard, S.; Brearley, A. J.; Remusat, L. Evolution of Organic Matter in Orgueil, Murchison and Renazzo during Parent Body Aqueous Alteration: In Situ Investigations. *Geochim. Cosmochim. Acta* **2014**, *131*, 368–392.

(31) Le Guillou, C.; Brearley, A. Relationships between Organics, Water and Early Stages of Aqueous Alteration in the Pristine CR3.0 Chondrite MET 00426. *Geochim. Cosmochim. Acta* **2014**, *131*, 344–367.

(32) Changela, H. G.; Le Guillou, C.; Bernard, S.; Brearley, A. J. Hydrothermal Evolution of the Morphology, Molecular Composition, and Distribution of Organic Matter in CR (Renazzo-Type) Chondrites. *Meteorit. Planet. Sci.* **2018**, *53*, 1006–1029.

(33) Wang, X.-C.; Lee, C. Adsorption and Desorption of Aliphatic Amines, Amino Acids and Acetate by Clay Minerals and Marine Sediments. *Mar. Chem.* **1993**, *44*, 1–23.

(34) Montgomery, W.; Tuff, J.; Kohn, S. C.; Jones, R. L. Reactions between Organic Acids and Montmorillonite Clay under Earth-Forming Conditions. *Chem. Geol.* **2011**, *283*, 171–176.

(35) Jaber, M.; Georgelin, T.; Bazzi, H.; Costa-Torro, F.; Lambert, J.-F.; Bolbach, G.; Clodic, G. Selectivities in Adsorption and Peptidic Condensation in the (Arginine and Glutamic Acid)/Montmorillonite Clay System. *J. Phys. Chem. C* **2014**, *118*, 25447–25455.

(36) Vinogradoff, V.; Le Guillou, C.; Bernard, S.; Viennet, J. C.; Jaber, M.; Remusat, L. Influence of Phyllosilicates on the Hydrothermal Alteration of Organic Matter in Asteroids: Experimental Perspectives. *Geochim. Cosmochim. Acta* **2020**, *269*, 150–166.

(37) Jaber, M.; Komarneni, S.; Zhou, C.-H. Synthesis of Clay Minerals. In *Handbook of Clay Science*; Bergaya, F., Lagaly, G., Eds.; Developments in Clay Science; Elsevier, 2013; Chapter 7.2, Vol. 5, pp 223–241.

- (38) Andrieux, P.; Petit, S. Hydrothermal Synthesis of Dioctahedral Smectites: The Al-Fe³⁺ Chemical Series: Part I: Influence of Experimental Conditions. *Appl. Clay Sci.* **2010**, *48*, 5–17.
- (39) Reinholdt, M.; Miehé-Brendlé, J.; Delmotte, L.; Le Dred, R.; Tuilier, M.-H. Synthesis and Characterization of Montmorillonite-Type Phyllosilicates in a Fluoride Medium. *Clay Miner.* **2005**, *40*, 177–190.
- (40) Vinogradoff, V.; Bernard, S.; Le Guillou, C.; Remusat, L. Evolution of Interstellar Organic Compounds under Asteroidal Hydrothermal Conditions. *Icarus* **2018**, *305*, 358–370.
- (41) Boogers, I.; Plugge, W.; Stokkermans, Y. Q.; Duchateau, A. L. Ultra-Performance Liquid Chromatographic Analysis of Amino Acids in Protein Hydrolysates Using an Automated Pre-Column Derivatisation Method. *J. Chromatogr. A* **2008**, *1189*, 406–409.
- (42) Aponte, J. C.; McLain, H. L.; Simkus, D. N.; Elsila, J. E.; Glavin, D. P.; Parker, E. T.; Dworkin, J. P.; Hill, D. H.; Connolly, H. C.; Lauretta, D. S. Extraterrestrial Organic Compounds and Cyanide in the CM2 Carbonaceous Chondrites Aguas Zarcas and Murchison. *Meteorit. Planet. Sci.* **2020**, DOI: 10.1111/maps.13531, in press.
- (43) Dworkin, J. P.; Adelman, L. A.; Ajluni, T.; Andronikov, A. V.; Aponte, J. C.; Bartels, A. E.; Beshore, E.; Bierhaus, E. B.; Brucato, J. R.; Bryan, B. H.; Burton, A. S.; Callahan, M. P.; Castro-Wallace, S. L.; Clark, B. C.; Clemett, S. J.; Connolly, H. C.; Cutlip, W. E.; Daly, S. M.; Elliott, V. E.; Elsila, J. E.; Enos, H. L.; Everett, D. F.; Franchi, I. A.; Glavin, D. P.; Graham, H. V.; Hendershot, J. E.; Harris, J. W.; Hill, S. L.; Hildebrand, A. R.; Jayne, G. O.; Jenkins, R. W.; Johnson, K. S.; Kirsch, J. S.; Lauretta, D. S.; Lewis, A. S.; Loiacono, J. J.; Lorentson, C. C.; Marshall, J. R.; Martin, M. G.; Matthias, L. L.; McLain, H. L.; Messenger, S. R.; Mink, R. G.; Moore, J. L.; Nakamura-Messenger, K.; Nuth, J. A.; Owens, C. V.; Parish, C. L.; Perkins, B. D.; Pryzby, M. S.; Reigle, C. A.; Richter, K.; Rizk, B.; Russell, J. F.; Sandford, S. A.; Schepis, J. P.; Songer, J.; Sovinski, M. F.; Stahl, S. E.; Thomas-Keperta, K.; Vellinga, J. M.; Walker, M. S. OSIRIS-REx Contamination Control Strategy and Implementation. *Space Sci. Rev.* **2018**, *214*, 19.
- (44) Cohen, S. A.; Michaud, D. P. Synthesis of a Fluorescent Derivatizing Reagent, 6-Aminoquinolyl-N-Hydroxysuccinimidyl Carbamate, and Its Application for the Analysis of Hydrolysate Amino Acids via High-Performance Liquid Chromatography. *Anal. Biochem.* **1993**, *211*, 279–287.
- (45) Glavin, D. P.; Dworkin, J. P.; Aubrey, A.; Botta, O.; Doty, J. H.; Martins, Z.; Bada, J. L. Amino Acid Analyses of Antarctic CM2 Meteorites Using Liquid Chromatography-Time of Flight-Mass Spectrometry. *Meteorit. Planet. Sci.* **2006**, *41*, 889–902.
- (46) Kopetzki, D.; Antonietti, M. Hydrothermal Formose Reaction. *New J. Chem.* **2011**, *35*, 1787–1794.
- (47) Ames, J. M. The Maillard Reaction. In *Biochemistry of Food Proteins*; Hudson, B. J. F., Ed.; Springer US, 1992; pp 99–153.
- (48) Weber, A. L. The Sugar Model: Catalysis by Amines and Amino Acid Products. *Origins Life Evol. Biospheres* **2001**, *31*, 71–86.
- (49) Brackman, W.; Smit, P. J. A New Synthesis of Nitriles. *Recl. Trav. Chim. Pays-Bas* **1963**, *82*, 757–762.
- (50) Oishi, T.; Yamaguchi, K.; Mizuno, N. Catalytic Oxidative Synthesis of Nitriles Directly from Primary Alcohols and Ammonia. *Angew. Chem., Int. Ed.* **2009**, *48*, 6286–6288.
- (51) Cleaves, H. J. The Prebiotic Geochemistry of Formaldehyde. *Precambrian Res.* **2008**, *164*, 111–118.
- (52) Cody, G. D.; Heying, E.; Alexander, C. M. O.; Nittler, L. R.; Kilcoyne, A. L. D.; Sandford, S. A.; Stroud, R. M. Establishing a Molecular Relationship between Chondritic and Cometary Organic Solids. *Proc. Natl. Acad. Sci. U.S.A.* **2011**, *108*, 19171–19176.
- (53) Aubrey, A. D.; Cleaves, H. J.; Bada, J. L. The Role of Submarine Hydrothermal Systems in the Synthesis of Amino Acids. *Origins Life Evol. Biospheres* **2009**, *39*, 91–108.
- (54) Yanagawa, H.; Kobayashi, Y.; Egami, F. Genesis of Amino Acids in the Primeval Sea: Formation of Amino Acids from Sugars and Ammonia in a Modified Sea Medium. *J. Biochem.* **1980**, *87*, 359–362.
- (55) Weber, A. L. Alanine Synthesis from Glyceraldehyde and Ammonium Ion in Aqueous Solution. *J. Mol. Evol.* **1985**, *21*, 351–355.
- (56) Kebukawa, Y.; Chan, Q. H. S.; Tachibana, S.; Kobayashi, K.; Zolensky, M. E. One-Pot Synthesis of Amino Acid Precursors with Insoluble Organic Matter in Planetesimals with Aqueous Activity. *Sci. Adv.* **2017**, *3*, No. e1602093.
- (57) Breslow, R. On the Mechanism of the Formose Reaction. *Tetrahedron Lett.* **1959**, *1*, 22–26.
- (58) Simonov, A. N.; Pestunova, O. P.; Matvienko, L. G.; Parmon, V. N. The Nature of Autocatalysis in the Butlerov Reaction. *Kinet. Catal.* **2007**, *48*, 245–254.
- (59) Palomo, C.; Aizpurua, J. M.; Ganboa, I.; Oiarbide, M. SS-Lactams as Versatile Intermediates in α - and β -Amino Acid Synthesis. *Synlett* **2001**, *2001*, 1813–1826.
- (60) Juršić, B. S.; Zdravković, Z. A Simple Preparation of Amides from Acids and Amines by Heating of Their Mixture. *Synth. Commun.* **1993**, *23*, 2761–2770.
- (61) Mitchell, J. A.; Reid, E. E. The Preparation Of Aliphatic Amides. *J. Am. Chem. Soc.* **1931**, *53*, 1879–1883.
- (62) Fu, X.; Liao, Y.; Glein, C. R.; Jamison, M.; Hayes, K.; Zaporski, J.; Yang, Z. Direct Synthesis of Amides from Amines and Carboxylic Acids under Hydrothermal Conditions. *ACS Earth Space Chem.* **2020**, *4*, 722.
- (63) Lambert, J. B.; Gurusamy-Thangavelu, S. A.; Ma, K. The Silicate-Mediated Formose Reaction: Bottom-Up Synthesis of Sugar Silicates. *Science* **2010**, *327*, 984–986.
- (64) Fuchida, S.; Masuda, H.; Shinoda, K. Peptide Formation Mechanism on Montmorillonite Under Thermal Conditions. *Origins Life Evol. Biospheres* **2014**, *44*, 13–28.
- (65) Schwartz, A. W.; de Graaf, R. M. The Prebiotic Synthesis of Carbohydrates: A Reassessment. *J. Mol. Evol.* **1993**, *36*, 101–106.
- (66) Botta, O.; Glavin, D. P.; Kminek, G.; Bada, J. L. Relative Amino Acid Concentrations as a Signature for Parent Body Processes of Carbonaceous Chondrites. *Origins Life Evol. Biospheres* **2002**, *32*, 143–163.
- (67) Hewins, R. H.; Bourot-Denise, M.; Zanda, B.; Leroux, H.; Barrat, J.-A.; Humayun, M.; Göpel, C.; Greenwood, R. C.; Franchi, I. A.; Pont, S.; Lorand, J.-P.; Cournède, C.; Gattacceca, J.; Rochette, P.; Kuga, M.; Marrocchi, Y.; Marty, B. The Paris Meteorite, the Least Altered CM Chondrite so Far. *Geochim. Cosmochim. Acta* **2014**, *124*, 190–222.
- (68) Lambert, J.-F. Adsorption and Polymerization of Amino Acids on Mineral Surfaces: A Review. *Origins Life Evol. Biospheres* **2008**, *38*, 211–242.
- (69) Busemann, H.; Young, A. F.; Alexander, C. M. O.; Hoppe, P.; Mukhopadhyay, S.; Nittler, L. R. Interstellar Chemistry Recorded in Organic Matter from Primitive Meteorites. *Science* **2006**, *312*, 727–730.
- (70) Zega, T. J.; Alexander, C. M. O. D.; Busemann, H.; Nittler, L. R.; Hoppe, P.; Stroud, R. M.; Young, A. F. Mineral Associations and Character of Isotopically Anomalous Organic Material in the Tagish Lake Carbonaceous Chondrite. *Geochim. Cosmochim. Acta* **2010**, *74*, 5966–5983.
- (71) Vinogradoff, V.; Le Guillou, C.; Bernard, S.; Binet, L.; Cartigny, P.; Brearley, A. J.; Remusat, L. Paris vs. Murchison: Impact of Hydrothermal Alteration on Organic Matter in CM Chondrites. *Geochim. Cosmochim. Acta* **2017**, *212*, 234.
- (72) Pizzarello, S.; Huang, Y. The Deuterium Enrichment of Individual Amino Acids in Carbonaceous Meteorites: A Case for the Presolar Distribution of Biomolecule Precursors. *Geochim. Cosmochim. Acta* **2005**, *69*, 599–605.
- (73) Yang, J.; Epstein, S. Relic Interstellar Grains in Murchison Meteorite. *Nature* **1984**, *311*, 544–547.
- (74) Glavin, D. P.; Dworkin, J. P. Enrichment of the Amino Acid L-Isovaline by Aqueous Alteration on CI and CM Meteorite Parent Bodies. *Proc. Natl. Acad. Sci. U.S.A.* **2009**, *106*, 5487–5492.

(75) Bruston, P.; Audouze, J.; Madjar, A. V.; Laurent, C. Physical and Chemical Fractionation of Deuterium in the Interstellar Medium. *Astrophys. J.* **1981**, *243*, 161–169.

(76) Oba, Y.; Takano, Y.; Naraoka, H.; Kouchi, A.; Watanabe, N. Deuterium Fractionation upon the Formation of Hexamethylenetetramines through Photochemical Reactions of Interstellar Ice Analogs Containing Deuterated Methanol Isotopologues. *Astrophys. J.* **2017**, *849*, 122.

Supplementary Information for

Impact of phyllosilicates on amino acid formation under asteroidal conditions

V. Vinogradoff^{1,2*}, L. Remusat², H.L. McLain^{3,4}, J.C. Aponte^{3,4}, S. Bernard², G. Danger^{1,5}, J.P. Dworkin³, J.E. Elsila³, and M. Jaber^{5,6}

¹Physique des Interactions Ioniques et Moléculaires, PIIM UMR-CNRS 7345, Aix-Marseille Université, 13397-Marseille, France

²Muséum National d'Histoire Naturelle, Sorbonne Université, UMR CNRS 7590, Institut de minéralogie, de physique des matériaux et de cosmochimie, Paris, France.

³Solar System Exploration Division, NASA Goddard Space Flight Center, Greenbelt, Maryland 20771, United States

⁴Department of Chemistry, The Catholic University of America, Washington, DC 20064, United States

⁵Institut Universitaire de France (IUF)

⁶Sorbonne Université, CNRS UMR 8220, LAMS, case courrier 225, 4 pl. Jussieu 75252 Paris cedex 05, France

* Corresponding author: Vassilissa Vinogradoff

Email: vassilissa.vinogradoff@univ-amu.fr

Supplementary Methods for smectite characterization.

X-ray diffraction analysis

The XRD patterns were collected at the X-ray diffraction facility of IMPMC (Paris, France). The X-ray powder diffraction patterns were recorded using an X'Pert Pro Panalytical diffractometer equipped with a $\text{CoK}\alpha_{1,2}$ radiation source ($\lambda\text{K}\alpha_1 = 1.78897 \text{ \AA}$, $\lambda\text{K}\alpha_2 = 1.79285 \text{ \AA}$) and an X'Celerator detector, in Bragg Brentano geometry (0.04° Soller slits, 0.5° programmable divergence slit, 1° incident antiscatter slit, and 0.5° diffracted antiscatter slit). The XRD patterns were collected between 3 and $60^\circ 2\theta$ with a step size of $0.0167^\circ 2\theta$ and a counting time per step of 6.7 s . Less than 0.5 mg of grounded samples were placed on a Si pellet and introduced in the diffractometer. The analysis on the pellet may have influenced the profile of diffraction pattern due to random geometry of the phyllosilicate.

Infrared spectroscopy analysis

FTIR analyses were performed using a Vertex 70 spectrometer (Bruker) at the Musée de l'Homme (Paris, France). Around 0.5 mg of powdered sample was pressed onto a diamond crystal surface using a single reflection in the attenuated total resonance device, ATR-quest (Specac). The spectrum was acquired from 370 to 4000 cm^{-1} with a spectral resolution of 4 cm^{-1} . Ninety-six spectra were accumulated (vs. 128 for the background). Each IR spectrum was corrected with a linear elastic concave baseline and normalized to its total absorbance area (using Bruker Opus software).

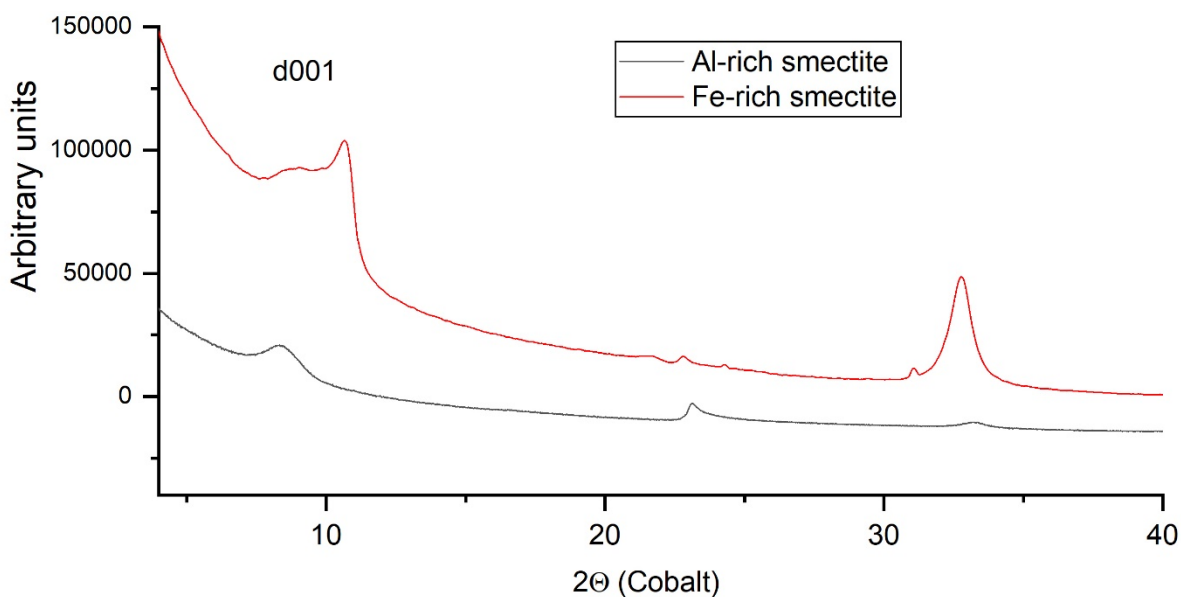
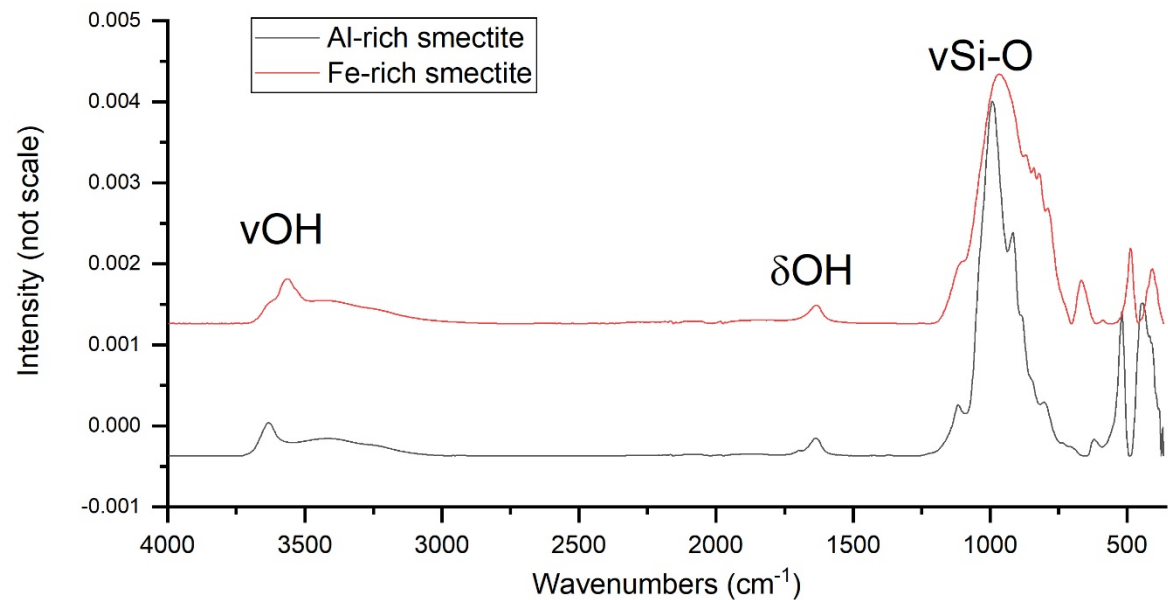


Figure S11 Infrared spectra and X-ray diffraction spectra of the synthetic smectites used in this study. Main IR band are indicated (νOH : stretching OH from smectite, δOH stretching from adsorbed water, $\nu\text{Si-O}$, stretching Si-O from smectite). On the XRD spectra is indicated the location of the d001 diffraction band corresponding to the interlayer space of smectites.

Table SII. Abundance of amino acid analyzed in the hydrothermal samples at 0, 2, 7 and 31 days (values are reported in μM with standard deviation errors over 3 analyses, see methods).

Exp.	Glycine	α -Alanine	β -Ala	γ -ABA	β -ABA	β -AIB	α -ABA	α -AIB	Total amino acids
HMT									
0 day	0.42 ± 0.10	<0.1	<0.1	<0.1	<0.1	<0.1	<0.1	<0.1	<0.5
2 days	7.67 ± 0.25	<0.1	0.96 ± 0.03	<0.1	<0.1	<0.1	<0.1	<0.1	9
7 days	190.64 ± 5.06	6.97 ± 0.86	7.91 ± 0.20	1.17 ± 0.24	0.59 ± 0.03	0.89 ± 0.19	<0.1	<0.1	208
31 days	573.44 ± 15.15	30.31 ± 2.11	15.35 ± 0.38	11.01 ± 2.88	1.22 ± 1.05	2.39 ± 0.77	1.22 ± 0.27	0.30 ± 0.23	635
HMT+CA									
0 day	20.90 ± 1.06	<0.1	<0.1	<0.1	<0.1	<0.1	<0.1	<0.1	21
2 days	53.43 ± 1.45	0.75 ± 0.10	2.15 ± 0.14	<0.1	<0.1	<0.1	<0.1	<0.1	57
7 days	399.59 ± 8.67	8.59 ± 0.63	14.96 ± 0.96	1.45 ± 0.26	0.66 ± 0.29	1.20 ± 0.25	1.19 ± 0.05	<0.1	428

31 days	396.82 ± 7.66	15.35 ± 1.46	18.22 ± 1.21	1.53 ± 0.25	0.71 ± 0.02	1.37 ± 0.31	1.18 ± 0.04	0.23 ± 0.12	436
HMT+Al- rich smectite									
0 day	1.56 ± 0.12	0.20 ± 0.02	<0.1	<0.1	<0.1	<0.1	<0.1	<0.1	2
2 days	96.98 ± 4.61	0.85 ± 0.07	4.38 ± 0.34	0.89 ± 0.07	<0.1	<0.1	<0.1	<0.1	103
7 days	149.57 ± 3.73	1.91 ± 0.15	6.04 ± 0.43	0.92 ± 0.14	0.59 ± 0.02	0.77 ± 0.08	<0.1	<0.1	160
31 days	1314.34 ± 16.90	57.40 ± 2.58	17.81 ± 0.69	73.01 ± 5.56	3.82 ± 3.09	2.05 ± 1.33	1.27 ± 0.07	0.25 ± 0.17	1470
HMT+Fe- rich smectite									
0 day	0.79 ± 0.06	0.44 ± 0.04	<0.1	<0.1	<0.1	<0.1	<0.1	<0.1	1
2 days	45.44 ± 0.77	0.73 ± 0.05	1.62 ± 0.81	<0.1	<0.1	<0.1	<0.1	<0.1	48
7 days	25.36 ± 0.48	1.01 ± 0.05	3.91 ± 0.24	0.89 ± 0.01	<0.1	<0.1	<0.1	<0.1	31
31 days	223.11 ± 5.70	10.39 ± 0.82	11.89 ± 0.90	20.13 ± 8.52	1.91 ± 1.05	1.69 ± 0.46	1.24 ± 0.09	0.08 ± 0.28	270

Table SI2. Amino acid yields for the four set of experiments after 31 days of hydrothermal reactions at 150 °C, pH 10 and the relative abundance order of the 4 main amino acids, gly: glycine, ala: alanine, β -ala: β -alanine, γ -ABA: γ -aminobutyric acid.

Initial Composition exp	Percent yield /HMT after 31 days, 150 °C	Amino acid formed
HMT	0.09	gly >> ala > β -ala > γ -ABA
HMT+CA	0.06	gly >> β -ala > ala > γ -ABA
HMT+Al-rich smectite	0.21	gly >> γ -ABA > ala > β -ala
HMT+Fe-rich smectite	0.038	gly >> γ -ABA > β -ala > ala

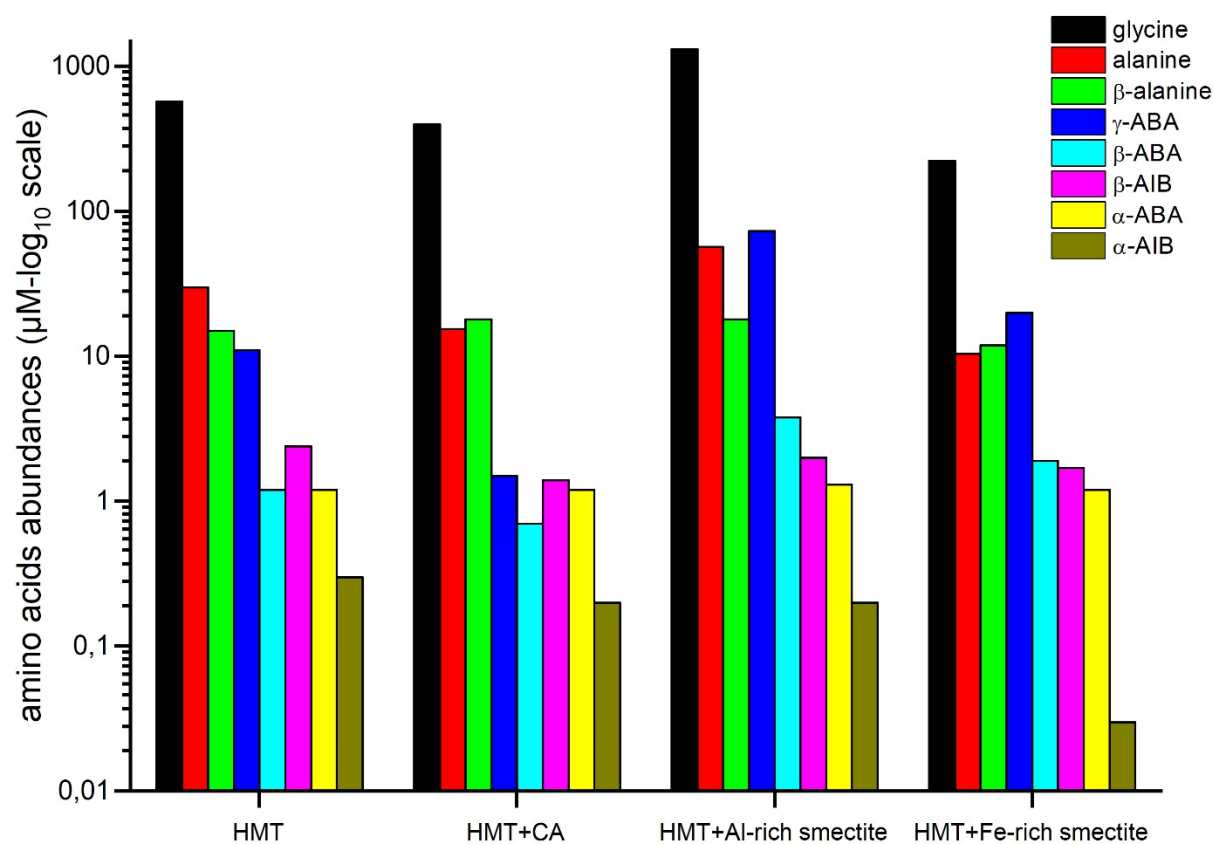


Figure S12. Bar graph of the nature and distribution of the amino acids formed in function of the experiments from HMT-only, HMT+CA, HMT+Al-rich smectite and HMT+Fe-rich smectite after 31 day long hydrothermal alteration experiments at 150°C. Scale are in \log_{10} to increase the visibility of the low abundant compounds.

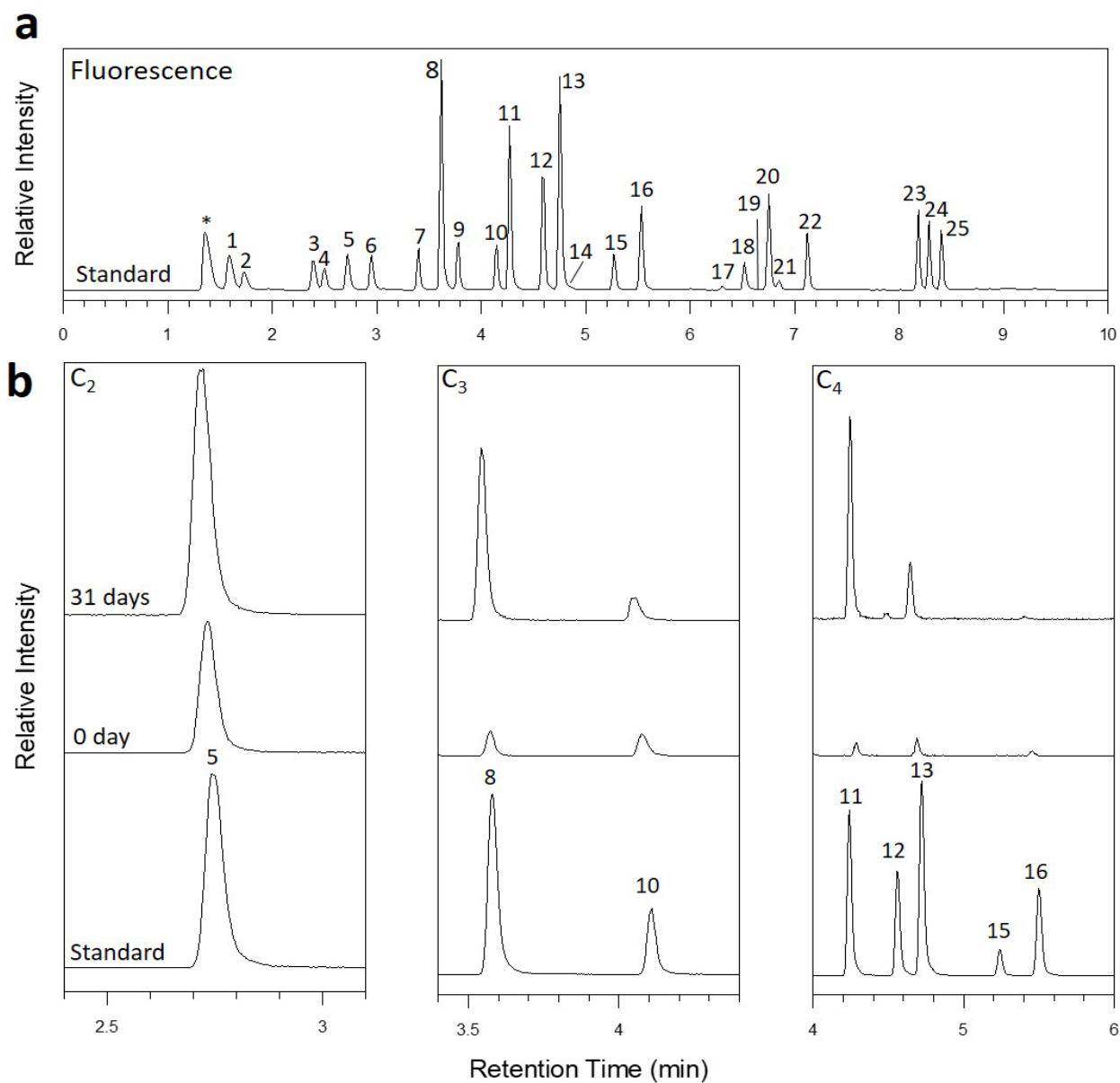


Figure SI3. Fluorescence chromatogram of the standard amino acids analyzed in this study (a) and zoom in the amino acids formed in the experiment with HMT-only after 31 days of hydrothermal alteration compared to the 0 day sample (unheated) (b). Scale has been maximized for clarity. Number referred to amino acid reported in table SI3 with their actual abundance. The * is a derivatization side product in the standard. Identification of the compounds is listed in Table SI3.

Table SI3. List of amino acid and their abundance in μM analyzed in the HMT-only sample after 0, 2, 7, and 31 days of hydrothermal alteration. Peaks refer to the numbers in Figure SI2.

Analyte	Peak	0 day	2 days	7 days	31 days
Ammonia	1				
Histidine	2	<0.1	<0.1	<0.1	<0.1
Serine	3	<0.1	<0.1	<0.1	<0.1
Arginine	4	<0.1	<0.1	<0.1	<0.1
Glycine	5	0.4 ± 0.1	7.7 ± 0.3	190.6 ± 5.1	573.4 ± 15.2
Aspartic acid	6	<0.1	<0.1	<0.1	<0.1
Glutamic acid	7	<0.1	<0.1	<0.1	<0.1
β -alanine	8	<0.1	1.0 ± 0.03	7.9 ± 0.2	15.4 ± 0.4
Threonine	9	<0.1	<0.1	<0.1	<0.1
Alanine	10	<0.1	<0.1	7.0 ± 0.9	30.3 ± 2.1
γ -amino butyric acid (γ -ABA)	11	<0.1	<0.1	1.2 ± 0.2	11.0 ± 2.9

DL- β -aminobutyric acid (DL- β -ABA)	12	<0.1	<0.1	0.6 \pm 0.03	1.2 \pm 1.1
DL- β -aminoisobutyric acid (DL- β -AIB)	13	<0.1	<0.1	0.9 \pm 0.2	2.4 \pm 0.8
Proline	14	<0.1	<0.1	<0.1	<0.1
α -aminoisobutyric acid (α -ABA)	15	<0.1	<0.1	<0.1	1.2 \pm 0.3
α -aminoisobutyric acid (α -AIB)	16	<0.1	<0.1	<0.1	0.3 \pm 0.2
Cysteine	17	<0.1	<0.1	<0.1	<0.1
Lysine	18	<0.1	<0.1	<0.1	<0.1
Tyrosine	19	<0.1	<0.1	<0.1	<0.1
ϵ -aminocaproic acid (ϵ -ACA)	20	<0.1	<0.1	<0.1	<0.1
Methionine	21	<0.1	<0.1	<0.1	<0.1
Valine	22	<0.1	<0.1	<0.1	<0.1
Leucine	23	<0.1	<0.1	<0.1	<0.1
Isoleucine	24	<0.1	<0.1	<0.1	<0.1
Phenylalanine	25	<0.1	<0.1	<0.1	<0.1

Supplementary text

Amides in the HMT+CA mixtures

Analysis by GC-MS

Compounds soluble in DCM were analyzed without derivatization, using an Agilent Technologies 6890N gas chromatograph coupled with an Agilent Technologies 5973 network mass spectrometer operated at the Laboratory Milieux Environnementaux, Transferts et Interactions dans les Hydrosystèmes et les Sols (METIS) in Paris, France. Description of the device is already described elsewhere (34, 35). The GC was equipped with a RTX-5Si/MS (30 m × 0.25 mm, 0.5 μm film) capillary column coated with chemically bound Restek (low-polarity phase, suitable for semi-volatile, hydrocarbon, amine, phenol compounds). The injection temperature was 280 °C in splitless mode and the GC oven programmed from 50 °C to 320 °C, ramping at 4 °C min⁻¹, and using He as gas carrier. The solvent delay was as short as possible (3 minutes). The mass spectrometer was operated at an electron energy of 70 eV, an ion source temperature of 220 °C and a scanning conditions from 35 to 700 amu at 2.24 scan s⁻¹. Products were identified using the NIST database. Data processing was done using the OpenChrom software, namely subtraction of the solvent background (DCM) taken at 3.8 min followed by an automatic peak detection using the MSD first derivative process (signal to noise ratios, S/N > 3).

Results

In the presence of carboxylic acids with HMT in the starting solution, additional organic compounds are observed with the ones already observed in the HMT-only experiments (34). These compounds appear between 5 and 11 minutes on the chromatograms and are assigned to amide

compounds, namely formamide, acetamide, and propanamide with N-methyl alkylation (Fig. SI4 and SI5, table SI4). The formation of some of these compounds may have inhibited the formation of other organic products, such as the one at 6.18, 6.6 or 7.8 min; which are not observed in the chromatogram. These compounds are N-heterocycles such as imidazoline, or pyrazoline with alkyl substitution, as discussed in Table 1 of Reference (34).

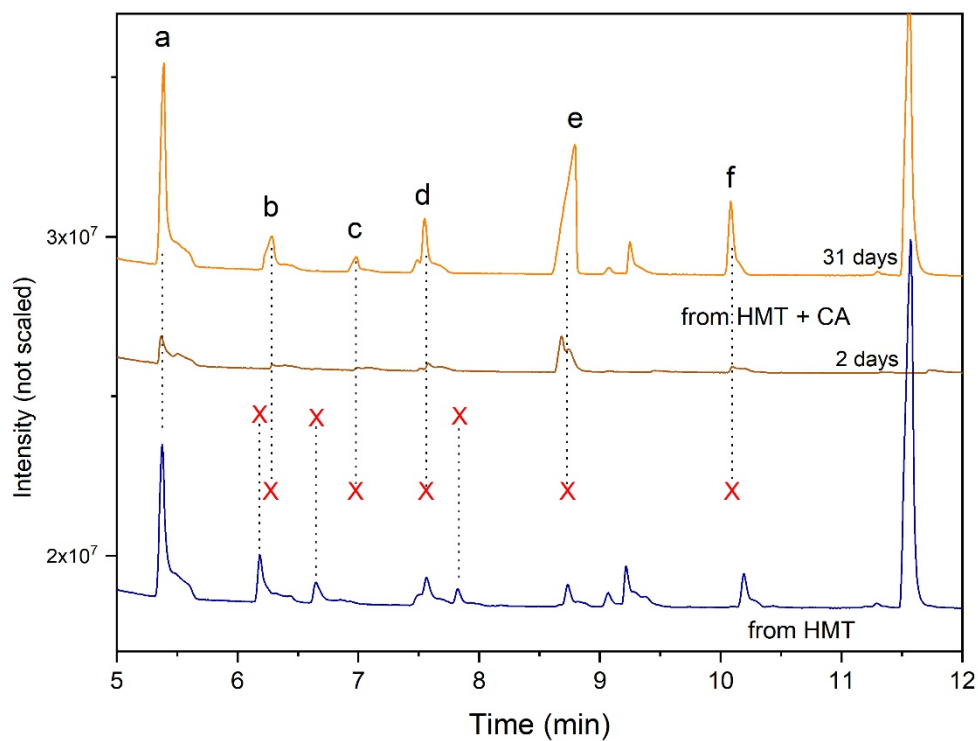
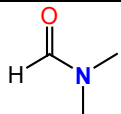
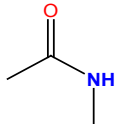
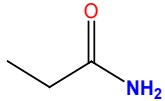
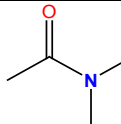
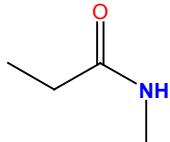
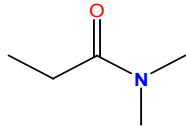


Figure SI4. GC-MS chromatograms of the DCM extract from the HMT+CA samples after 2 and 31 days of hydrothermal reaction, compared to the chromatogram from HMT alone after 31 days hydrothermal reaction (34). The lines ending by a red cross indicate the peaks present in the HMT+CA mixtures but not in the HMT-only mixture and reciprocally.

Table S14. Amides identified by GC-MS after 31 day long of hydrothermal experiments from the starting HMT+CA (0.7 M). See Figure S15 for the total mass spectrum of each amides. See Vinogradoff et al. (34) for identification of the rest of peaks in the chromatogram.

Figure SI3 label	Retention time	[M+]	Designation		Structures
			name	formula	
a	5.37	73	N,N-dimethyl formamide	C ₃ H ₇ NO	
b	6.27	73	N-methyl acetamide	C ₃ H ₇ NO	
c	6.97	73	propanamide	C ₃ H ₇ NO	
d	7.55	87	N,N-dimethyl acetamide	C ₄ H ₉ NO	
e	8.75	87	N-methyl propanamide	C ₄ H ₉ NO	

f	10.07	101	N,N-dimethyl propanamide	C ₅ H ₁₁ NO	
---	-------	-----	-----------------------------	-----------------------------------	---

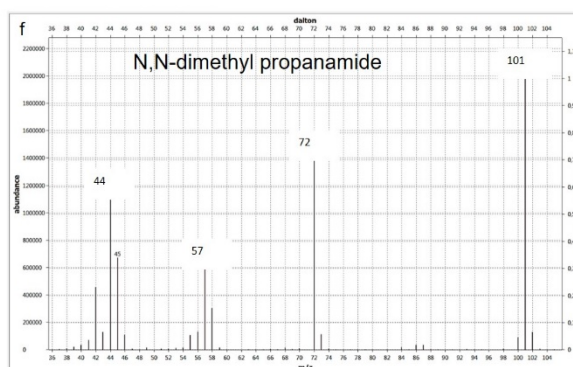
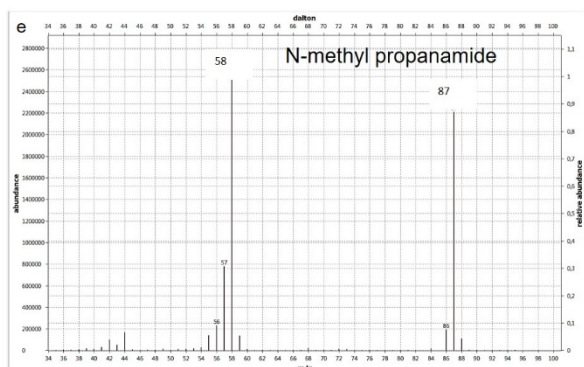
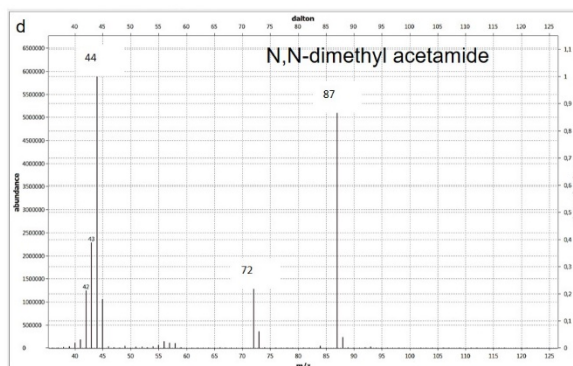
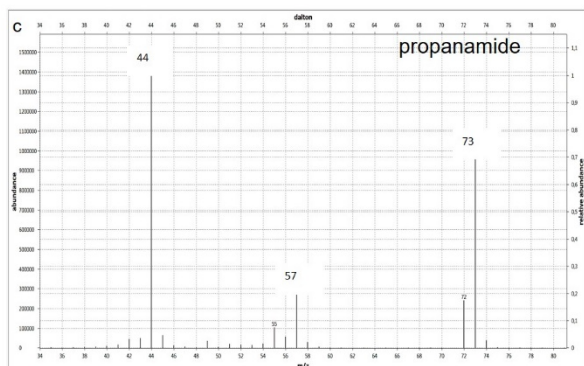
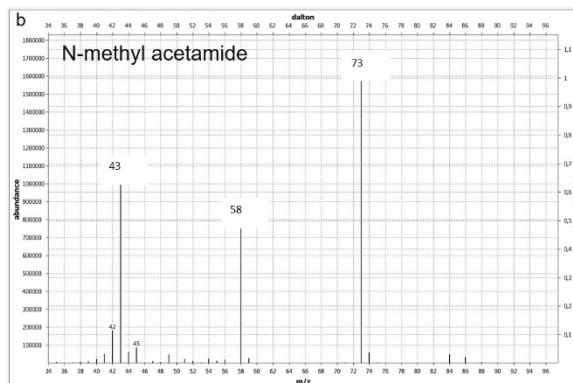
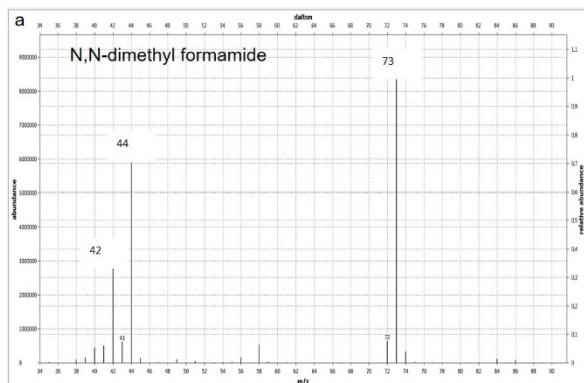


Figure SI5 Mass spectra of the compounds a to f labelled in figure SI4 corresponding to amides reported in Table SI4. m/z of the major peaks are reported for clarity.